Fine separation of particles via the entropic splitter

Yongge Li,[1] Yong Xu,[1,3,4,*] Wei Xu,[1] Zichen Deng,[1,2] and Jürgen Kurths[3,4]
[1]*Department of Applied Mathematics, Northwestern Polytechnical University, Xi'an 710072, China*
[2]*School of Mechanics, Civil Engineering and Architecture, Northwestern Polytechnical University, Xi'an 710072, China*
[3]*Potsdam Institute for Climate Impact Research, Potsdam 14412, Germany*
[4]*Department of Physics, Humboldt University Berlin, 12489 Berlin, Germany*
(Received 30 June 2017; published 25 August 2017)

We investigate the fine separation of particles with different sizes in an asymmetric confined channel by directing them moving to the opposite directions. Besides redesigning the geometry of the channel, we add a general rectangular wave oscillating force to enlarge the velocity differences between particles with different radii, which is important to increase the separation speed and sort particles of similar radii. The separation process is guaranteed by choosing a small period of the oscillating force and a proper partition strategy of the device length sifting particles to the left and right. The optimal set of parameters for a fixed amplitude of the oscillating force is found by the above regime. We show that by this regime the separation efficiency is significantly improved compared to the classic square wave force.

DOI: 10.1103/PhysRevE.96.022152

Matter consisting of masses of various small parts is widely seen in natural systems and industrial productions, e.g., mixed bacteria [1], designed nanoparticles within certain range [2], various DNA fragments [3,4], different kinds of cells [5,6], or more generally, mixtures of size-dispersed substances in liquids on a range from macroscale to nanoscale [7–9], to name but a few. To separate the wanted pure substances or distributed components from the mixtures is highly important in laboratory research and industrial manufacture. The particle separation techniques use arrays of obstacles [10,11], centrifuge machine [12,13], sieve or membrane [14–16], or external fields [17,18] to achieve the wanted separation by utilizing different responses of particles to the external device, which are based on properties such as the density, mass, size, surface charge, or magnetization.

Among these separation methods, the sorting of size-dependent particles is a challenge in chemistry, biology, nanotechnology, and industry. It is especially crucial for fine separation, which demands the capability of filtering particles with similar sizes, e.g., separating certain nanoparticles from nanosize mixture [19], or separating erythrocyte from blood [20]. A purely size-dependent fine separation traditionally uses a sieve or porous media, which require multilevel facilities to realize the crude sorting. To further separate the wanted from the similar size unwanted mixtures needs, however, more rigorous devices. This makes it difficult and costly to achieve fine separation. Thus the fine separation is strongly limited to the device. A low hardware-dependent mechanism or device is very necessary and constructively useful.

Recently, a low hardware-dependent separation mechanism was presented, i.e., the entropic splitter [21–23], which contains an asymmetric channel to induce the entropic rectification, an unbiased oscillating force to enlarge the rectified differences for particles, and a static force to control the moving direction. The particles of different radii are separated depending on differences of mean velocities induced by the interplay of the confinement and periodic force. However, the efficiency of the entropic splitter favors separating small particles from large particle mixtures, while it is tough to handle mixtures consisting of large particles of similar radii. The velocities of large particles stay so close that the velocity differences are not distinct enough to separate them fast. For example, it will take more than 10 times longer to separate particles of $r = 0.05$ from $r = 0.07$ than $r = 0.01$ when the amplitude of the oscillating force is 50 [21].

In this paper, we overcome this restriction by redesigning the geometry and changing the form of the external oscillating force to maximize the rectified differences for particles of various radii. This leads to large disparities of the velocity, which determine the separation speed and purity. Note that although for large amplitudes of the oscillating force the transport velocities are large, it does not say anything on the separation, whereas what counts here is the differences between the velocities of these particles to be separated.

We start by considering the imposed two-dimensional (2D) periodic channel, confining spherical Brownian particles of radius r suspended in a solvent of dynamic viscosity ν. This generates rich dynamical phenomena and has various potential applications in ion channel, microfluidic systems and nanoporous materials [24–27]. The confined periodic walls are mirror symmetric along the x direction given by $y = \tilde{\omega}_u(x) = -\tilde{\omega}_l(x)$ [Fig. 1(a)]. The geometry is defined by the upper boundary $\tilde{\omega}_u(x)$

$$\tilde{\omega}_u(x) = \begin{cases} b + k_1\overline{x}, & \overline{x} < L_2, \\ b + k_2(L - \overline{x}), & \text{else}, \end{cases} \tag{1}$$

where $\overline{x}$ is the modulo function $\overline{x} = \mathrm{mod}(x, L)$. $k_1 = h/L_1$, and $k_2 = h/L_2$ are the slopes of the left and right walls, respectively, $(h + b)$ and b refer to half of the maximum and minimum channel width respectively. To control the symmetry of the channel along the y direction, an adjustable parameter q is introduced satisfying $L_1 - L_2 = qL$ and $L_1 + L_2 = L$. When a hard-sphere particle of radius r transports in the confinement, its center will be restricted to access to the walls and channel angles, so the effective boundary is an

*Corresponding author: hsux3@nwpu.edu.cn

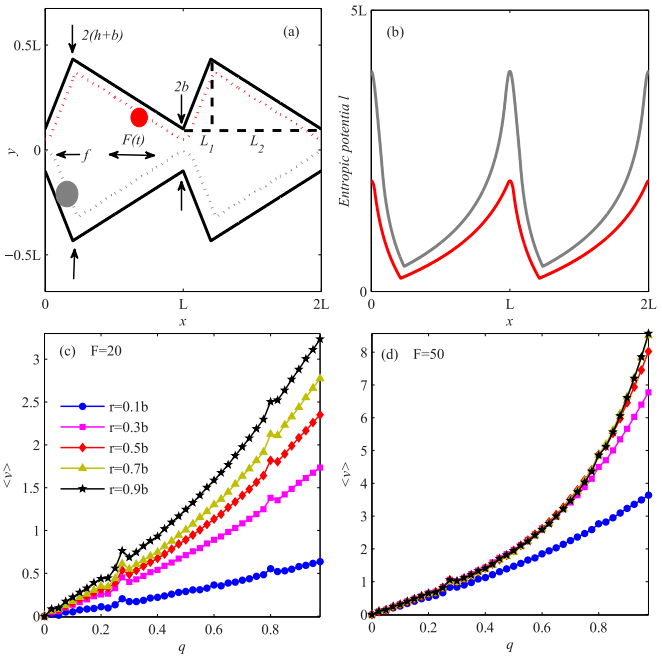

FIG. 1. Schematic diagram of the channel and the influence of the geometric parameter q. (a) The channel walls are defined by Eq. (1). The imaginary lines illustrate the effective boundaries confining the motion of sphere particles according to Eq. (2), driven by a static force f and a rectangular wave force $F(t)$. The parameters are set $q = 0.6, h = (0.1 + 1/3)L, b = 0.1L$. (b) The entropic potentials corresponding to the red and gray spheres in (a) defined by $-\ln[2\omega(x)]$. (c), (d) The mean velocities for particles of different radii with respect to q excited by a common square wave force $F(t) = F_0\mathrm{sgn}[\sin(2\pi t/\tau_p)]$ in the absence of a static force, for $F_0 = 20.0$ and $F_0 = 50.0$, respectively, $\tau_p = 20.0$. Symbol indicators corresponding to particles of different radii in (c) hold the same throughout the paper.

r-dependent reachable space inside the channel. The upper effective boundary reads then

$$\omega_u(x) = \begin{cases} b - \sqrt{r^2 - \overline{x}^2}, & 0 \leqslant \overline{x} < p_l, \\ b + k_1\overline{x} + r\sqrt{1+k_1^2}, & p_l \leqslant \overline{x} < p_b, \\ b + k_2(L - \overline{x}) - r\sqrt{1+k_2^2}, & p_b \leqslant \overline{x} < p_r, \\ b - \sqrt{r^2 - (L-\overline{x})^2}, & p_r \leqslant \overline{x} < L, \end{cases} \tag{2}$$

where $p_l = rk_1/\sqrt{1+k_1^2}$, $p_r = L - rk_2/\sqrt{1+k_2^2}$, and $p_b = L_1 + r[\sqrt{1+k_1^2} - \sqrt{1+k_2^2}]/(k_1+k_2)$. The lower effective boundary is given by $\omega_l(x) = -\omega_u(x)$.

We consider a particle of radius r in the channel and assume that (i) the particle suspension is dilute [26,28], and (ii) the reflecting boundary condition is fulfilled at the channel walls [29]. Under these assumptions effects caused by particle-particle interactions and particle-wall interactions can be safely neglected. The dynamic model exerted by an static force f and an external oscillating force $F(t)$ along the x direction can be described by the Langevin equation as

$$\gamma_r \frac{d\vec{\boldsymbol{r}}}{dt} = -[f + F(t)]\vec{\boldsymbol{e}}_{\boldsymbol{x}} + \sqrt{\gamma_r \kappa_B T}\vec{\boldsymbol{\xi}}(t), \tag{3}$$

where γ_r is the friction coefficient satisfying the Stokes' law $\gamma_r = 6\pi\nu r$, depending on the particle radius r and the viscosity ν of the fluid. $\vec{\boldsymbol{r}} = (x, y)$ is the position vector of the particle center, f is a static force, $\vec{\boldsymbol{e}}_{\boldsymbol{x}}$ is the unit vector along the x direction, k_B is the Boltzmann constant, and T denotes the absolute temperature. $\vec{\boldsymbol{\xi}}(t)$ is a Gaussian white noise with zero mean and unit variance $\langle \xi_x(t)\xi_y(t')\rangle = 2\delta_{x,y}(t - t')$.

Instead of the commonly used square wave form, we apply a general alterable rectangular wave force $F(t)$

$$F(t) = \begin{cases} \tilde{F}_0, & n\tau_p \leqslant t < n\tau_p + \tau_c, \\ -c\tilde{F}_0, & n\tau_p + \tau_c \leqslant t < (n+1)\tau_p, \end{cases} \tag{4}$$

where τ_p and τ_c are designed to satisfy that the temporal average of $F(t)$ over a period τ_p is zero, which requires the coefficient c to follow $\tau_c = c\tau_p/(1 + c)$. By changing c the rectangular wave is able to achieve various forms. When $c = 1$, $F(t)$ is similar to the classic square wave form $F(t) = \tilde{F}_0\mathrm{sgn}[\sin(2\pi t/\tau_p)]$.

For the sake of a dimensionless description, we rescale the length variables by L and the time variables by $\tau = 6\pi\nu b L^2/(k_B T)$ for the largest transportable particle of radius b. Then the Langevin equation is rewritten in a form involving dimensionless variables $t \to \hat{t}\tau$, $\tau_p \to \hat{\tau}_p\tau$, $\omega_u \to \hat{\omega}_u L$, $\omega_l \to \hat{\omega}_l L$, $x \to \hat{x}L$, $y \to \hat{y}L$, and $b \to \hat{b}L$. The scaled forces are $f \to \hat{f}k_B T/L$ and $F(t) \to \hat{F}(\tau)k_B T/L$. We assume that the external force is proportional to the radius r, i.e., $f = f_0 r/b$ and $\tilde{F}_0 = F_0 r/b$. After rescaling, Eq. (3) can be rewritten in a dimensionless form, for which we shall omit the hat symbols

$$\frac{d\vec{\boldsymbol{r}}}{dt} = -[f_0 + F(t)]\vec{\boldsymbol{e}}_{\boldsymbol{x}} + \sqrt{b/r}\vec{\boldsymbol{\xi}}(t), \tag{5}$$

where

$$F(t) = \begin{cases} F_0, & n\tau_p \leqslant t < n\tau_p + \tau_c, \\ -cF_0, & n\tau_p + \tau_c \leqslant t < (n+1)\tau_p. \end{cases}$$

Brownian particles in a 1D ratchet are able to exhibit a directional motion rectified by the asymmetry of the potential [9,30,31]. This phenomenon also happens in flashing, porous materials and corrugated channels because of the resulting asymmetric entropic potential like Fig. 1(b) due to the confinement. To evaluate influences of the asymmetric geometry, we fix the maximum and minimum width and vary q. The transport quantity of mean velocity $\langle v\rangle = \lim_{t\to\infty} \langle x(t)\rangle/t$ is simulated by averaging over an ensemble of 10^3 trajectories based on Eq. (5) via the standard stochastic Euler algorithm. In Figs. 1(c), 1(d) the mean velocities $\langle v\rangle$ increase for all particles with the increase of q. For a small force $F_0 = 20.0$, $\langle v\rangle$ of different radii are dispersed, i.e., the velocity differences of particles with adjacent radii are distinctive, which is a basic condition to achieve separation. However, for a large force $F_0 = 50.0$, only the velocity of particle $r = 0.1b$ is really distinctive. The other $\langle v\rangle$ are intertwined, which makes it extremely slow and difficult to separate large particles with similar radii. However, it should be noticed that a larger q will induce relatively larger

velocity differences. Hence the velocity lines tend to disperse with the increase of q. Thus a relative large $q = 0.9$ is chosen in the rest of this paper.

However, only depending on the geometry of the channel is not enough to sufficiently tap the potential of the entropic splitter, so besides q, the form of $F(t)$ should be considered too. A theoretical description of the influence of $F(t)$ can be obtained from the Fick-Jacobs (FJ) equation [32–34],

$$\frac{\partial P(x,t)}{\partial t} = \frac{\partial}{\partial x}\left\{D(x)\left[\frac{\partial P(x,t)}{\partial x} + V'(x)P(x,t)\right]\right\}, \quad (6)$$

where $V(x) = [f_0 + F(t)]x - \ln[2\omega(x)]$. In the adiabatic limit, the mean velocity is given as

$$\langle v\rangle = \frac{c}{1+c}J(F_0) + \frac{1}{1+c}J(-cF_0), \quad (7)$$

where the current J is

$$J(F_0) = \frac{1 - e^{-(F_0+f_0)r/b}}{\int_{x_0}^{x_0+1}\frac{1}{D(z)}e^{V(z)}\,dz\int_{z-1}^{z}e^{-V(x)}\,dx},$$

while $D(x) = b/\{r[1+\omega(x)^2]^{1/3}\}$ is the diffusion coefficient.

To separate particles, one key point is the velocity difference, i.e., $\Delta\langle v\rangle = |\langle v\rangle_{r_1} - \langle v\rangle_{r_2}|$, instead of the transport speed $\langle v\rangle$. The separated particles will go away from each other in a total speed of $\Delta\langle v\rangle$, so the larger the $\Delta\langle v\rangle$ the faster the separation. In Eq. (7), $\langle v\rangle$ is divided into two parts by the parameter c, which influences not only the proportion but also the value of the negative current $J(-cF_0)$. By tuning c the negative current will counteract the positive flux, which will evolve into diverse results rather than a single square wave case $\langle v\rangle = 1/2[J(F_0) + J(-F_0)]$.

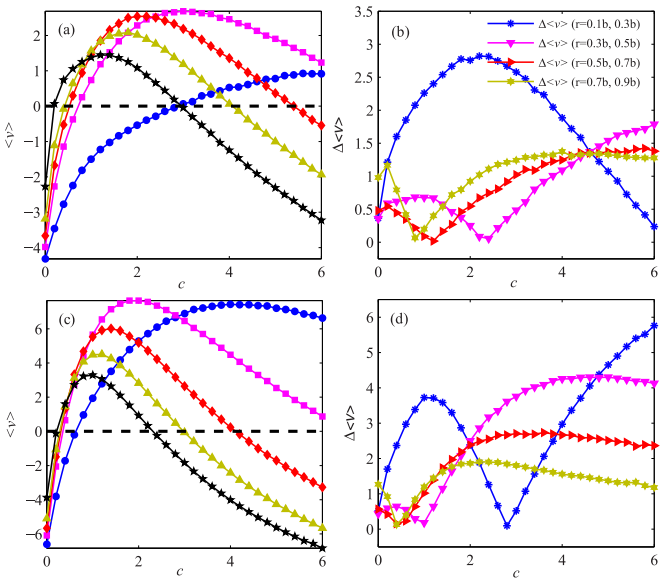

FIG. 2. Influences of c on the mean velocity $\langle v\rangle$ and the corresponding differences for $q = 0.9$ and $\tau_p = 4.0$. (a) $\langle v\rangle$ vs c for $F_0 = 50.0$ and $f_0 = -6.5$. (b) The corresponding absolute values of $\Delta\langle v\rangle$ between particles of similar radii in (a), i.e., $\Delta\langle v\rangle$ between $r = 0.1b$ and $r = 0.3b$, $r = 0.3b$ and $r = 0.5b$, $r = 0.5b$, and $r = 0.7b$, $r = 0.7b$, and $r = 0.9b$. (c) $\langle v\rangle$ vs c for $F_0 = 100.0$ and $f_0 = -9.5$. (d) The corresponding absolute values of $\Delta\langle v\rangle$ between particles of similar radii in (c), the legend instructions is the same as (b).

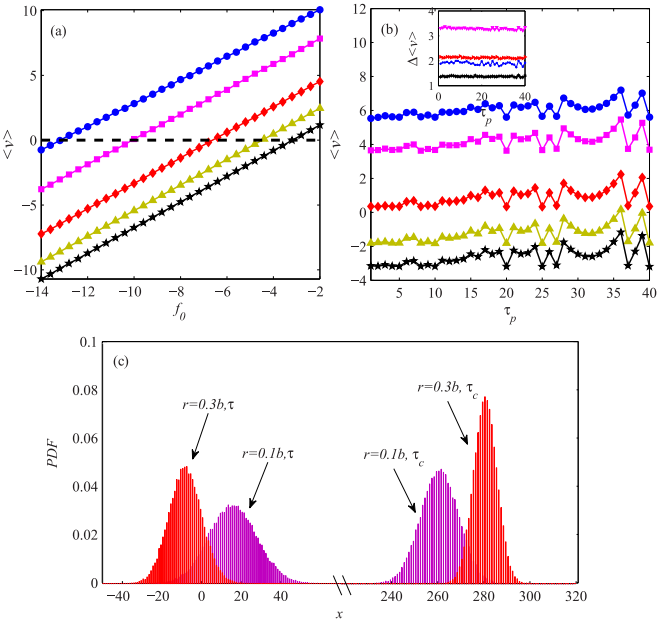

FIG. 3. Mean velocity with respect to the static force f_0 and the period τ_p for $q = 0.9$. (a) $\langle v\rangle$ vs f_0 to control the moving directions and tune the velocity allocation to two directions, $F_0 = 80.0$. (b) $\langle v\rangle$ as a function of the period τ_p for particles of diverse radii for $q = 0.9$ and $F_0 = 80.0$, inset: the absolute values of velocity difference between particles of adjacent radii, blue star for $r = 0.1b$ and $r = 0.3b$, purple inverted triangle for $r = 0.3b$ and $r = 0.5b$, red right-pointing triangle for $r = 0.5b$ and $r = 0.7b$, the black hexagram for $r = 0.7b$ and $r = 0.9b$. (c) The evolution of the probability density function (PDF) in the first τ_p for $F_0 = 100.0$ and $f_0 = -13.2$.

Figure 2 shows $\langle v\rangle$ vs c for particles of different radii, and the corresponding differences between particles of adjacent r at the two external force levels. For both cases, except $r = 0.1b$, the critical velocity points from increasing to decreasing tend to be smaller for larger particles, which induces a varying $\Delta\langle v\rangle$ among different particles. In Fig. 2(a), $\langle v\rangle$ at $c = 1$ are apparently staying close, that only $r = 0.1b$ can be distinctly separated from other particles, while it is tough for others. With the increase of c, $\langle v\rangle$ become more dispersive, hence c actually affects much in the separation. Figure 2(b) shows $\Delta\langle v\rangle$ between particles of adjacent radii. As shown on the limited x axis, the difference between particles $r = 0.1b$ and $r = 0.3b$ has a maximum at about $c = 2.2$, which is a better choice than others. Similarly, within the panel $c = 6.0$ for $r = 0.3b$ and $r = 0.5b$, $c = 4.0$ for $r = 0.7b$ and $r = 0.9b$. So with a fixed F_0, we can always find an optimal value c maximizing the $\Delta\langle v\rangle$. For larger $F_0 = 100.0$ in Figs. 2(c), 2(d) $c = 1.0$ is still not the best choice for each case, while all the maxima of $\Delta\langle v\rangle$ increase, i.e., we can speed up the separation by increasing F_0. To illustrate how to separate particles, look at Fig. 2(c) for example. If one wants to separate two similar particles such as $r = 0.3b$ and $r = 0.5b$, c can be chosen at 5.0. Then particles of radius $r = 0.3b$ move to the right with $\langle v\rangle = 2.54$, whereas particles of radius $r = 0.5b$ go to the left with $\langle v\rangle = -1.7$.

The best way to separate two kinds of particle is letting them move to the opposite directions. To achieve this, a static force f_0 should be added to manipulate the transport. Figure 3(a)

gives $\langle v\rangle$ vs the static force f_0 for $F_0 = 80.0$. Fortunately, the velocities are almost parallel and depend linearly on f_0. Hence the change of f_0 will lead to a vertical shift for all particles in Figs. 2(a) and 2(c), $f_0 > 0$ leading to shifting up and $f_0 < 0$ to shifting down. This provides an efficient control of separation and guarantees that particles of different radii move in the opposite directions with the same or similar speed.

Although F_0 can speed up the separation process, it does not mean that F_0 can be infinitely large, especially for large τ_p because at the beginning [Fig. 3(c)], positive current $J(F_0)$ will strongly drive particles to the right in τ_c. If F_0 and τ_c are both too large, particles will probably flow out into the right collector before the negative current $J(-cF_0)$ pushes them back. To avoid such a faulty operation, either a small F_0 or a long separation device is an appropriate choice.

However, it is still the best to use a short device and a large F_0 to save the device cost and keep a high separation speed. So we suggest lowering the period τ_p in order to reduce the right progressing duration τ_c of $F(t)$, which results into a limited moving distance in each step and keeps away a wrong exiting. Figure 3(b) shows $\langle v\rangle$ vs the oscillating period τ_p for different particles. We are excited to see that starting from $\tau_p = 1.0$ with increasing of τ_p although $\langle v\rangle$ slowly increases with fluctuations, the $\Delta\langle v\rangle$ between adjacent radii are almost unchanged [see the inset in Fig. 3(b)]. Thus τ_p influences slightly the separation speed for $1.0 \leqslant \tau_p \leqslant 40.0$, and we can choose a relative small period, such as $\tau_p = 4.0$, to avoid a wrong flowing, while keep the separation speed.

For the device, a common practice is placing mixtures in the middle of the device ($L_r = L_l$), and adjusting the parameters to let $\langle v\rangle_r \approx -\langle v\rangle_l$ for $\langle v\rangle$ to the right and left, respectively. This operation is adopted in most related work. As seen in Fig. 3(c) particles going to the right will first proceed a long distance $J(F_0)\tau_c$ and then go back with a gap $\tau_p\langle v\rangle$. To reach the right collector, particles will have to go through several forward and backward movements until the rest distance is within the range $|J(-cF_0)|(\tau_p - \tau_c) < L_x < J(F_0)\tau_c$, as shown in the illustration Fig. 4. The situation for particles going to the left is simpler. They will move forward and backward until shifting to the left collector. The arrival times are $t_r = L_x/J(F_0) + (L_r - L_x)/\langle v\rangle_r$ and $t_l \approx L_l/|\langle v\rangle_l|$. Because L_x is large, if $L_r = L_l$ the arrival times for two directions will vary strongly. The right collector will be instilled first and then we have to wait a long time for the arrival of the left-going particles. To get particles in two collectors simultaneously, i.e., $t_r = t_l$, we have

$$L_l = \frac{|\langle v\rangle_l|(NL - L_x) + \langle v\rangle_r|\langle v\rangle_l|L_x/J(F_0)}{\langle v\rangle_r + |\langle v\rangle_l|},$$
$$L_r = NL - L_l, \tag{8}$$

in which we can approximate $L_x \approx J(F_0)\tau_c$, and the induced time error is within τ_c.

To examine the splitter, specific examples under various combinations are tested. We set $F(t)$ a small period $\tau_p = 4.0$ to guarantee that the particles will not exit either side within the first τ_c interval. This ensures that all particles experience several periods before coming out. The channel is assumed to have a total length of $NL = 10^3 L$, and the partition for the left and right is based on Eq. (8). We use 2×10^4 mixed particles of two different radii to evaluate the efficiency, and the particles are initially uniformly distributed in the joint interval at $t = 0$. The procedure is repeated 40 times to get a mean separation time. As can be seen in Table I, with larger force F_0 the separation speed is faster, as expected from the previous discussions. The arrival time for different partitions is obvious smaller than in the case $L_r = L_l$. More importantly, the two kinds of particles always achieve a perfect purity 100%.

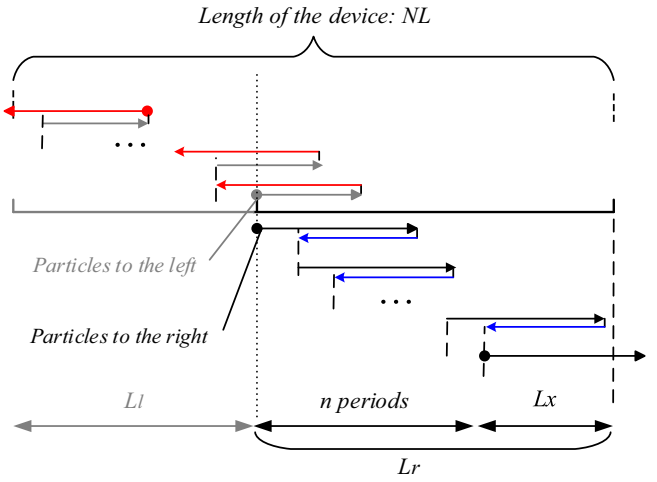

FIG. 4. Illustration of the transport for particles to the left and right. The total length of the device is NL, the divided partition for the left is L_l, and the right L_r includes two parts $n\tau_p\langle v\rangle_r$ and L_x.

In summary, we have proposed a flexible and efficient procedure, which is capable of optimizing the entropic splitter and achieving fine separation of particles of rather similar radii. We have found that with increasing the steepness of the channel walls, the velocities of different particles tend to disperse, which indicates that a large q is beneficial to the separation process. Besides the geometrical properties, we have demonstrated that the form of the oscillating driving force does affect the separation deeply. This enables us to design an optimal form of $F(t)$ to achieve a fine separation fast and purely. The particles can be controlled to move in the opposite directions by tuning the static force. To avoid particles exiting

TABLE I. The mean separation time for the parameters $q = 0.9$ and $\tau_p = 4.0$, that all experimental particles of r_1 and r_2 with the same number 10^4, initially uniformly distributed in the joint interval, reach the collectors, respectively. In the time row, M corresponds to the arrival time when $L_r = L_l$, and P corresponds to the arrival time based on Eq. (8). L_r is the length of the right separation part and $(10^3 L - L_r)$ is the left case which does not appear in the Table.

r_1	r_2	F_0	f_0	c	Time (M/P)	L_r
$0.1b$	$0.3b$	100	−13.4	6.0	160.9 s/129.8 s	$621L$
$0.3b$	$0.5b$	100	−10.6	4.6	221.2 s/175.0 s	$642L$
$0.5b$	$0.7b$	100	−9.2	3.6	338.2 s/276.5 s	$645L$
$0.7b$	$0.9b$	100	−10.7	2.2	465.4 s/410.0 s	$640L$
$0.1b$	$0.3b$	150	−16.9	6.0	85.2 s/56.2 s	$696L$
$0.3b$	$0.5b$	150	−15.5	3.2	150.5 s/99.0 s	$693L$
$0.5b$	$0.7b$	150	−13.4	2.4	244.0 s/167.8 s	$689L$
$0.7b$	$0.9b$	150	−14.0	1.6	374.8 s/284.6 s	$677L$

from the wrong direction, while keeping a high separation speed and using a short length of the device, we suggest reducing the period τ_p of $F(t)$ to limit the moving distance in the first τ_c. We have shown that for $1.0 \leqslant \tau_p \leqslant 40.0$ the velocity differences of particles of adjacent radii almost keep unchanged. Thus a small $\tau_p = 4.0$ is used, which proves to be effective. We have proposed a strategy that leads to a partition of the length for the left and right device. This solves the problem that we have to wait long for the left collector after obtaining the right one. The fine separation efficiency can be increased by using many channels in parallel. Nevertheless, due to the ideal assumptions there are still open questions about the efficiency and control before an implementation of practical experiments.

This work was supported by the National Natural Science Foundation of China (Grants No. 11372247, No. 11772255), the Fundamental Research Funds for the Central Universities, and the Innovation Foundation for Doctoral Dissertation of NPU.

[1] R. G. Harrison *et al.*, *Bioseparation Science and Engineering* (Oxford University Press, New York, 2003).
[2] M. Ploschner *et al.*, Nano Lett. **12**, 1923 (2012).
[3] K. D. Dorfman, Rev. Mod. Phys. **82**, 2903 (2010).
[4] J. S. Bader *et al.*, Proc. Natl. Acad. Sci. USA **96**, 13165 (1999).
[5] T. M. Geislinger and T. Franke, Biomicrofluidics **7**, 044120 (2013).
[6] J. Voldman, Annu. Rev. Biomed. Eng. **8**, 425 (2006).
[7] A. Corma, Chem. Rev. **97**, 2373 (1997).
[8] R. J. Wakeman and E. S. Tarleton, *Solid/Liquid Separation: Scale-Up of Industrial Equipment* (Elsevier Advanced Technology, Oxford, 2005).
[9] P. Hänggi and F. Marchesoni, Rev. Mod. Phys. **81**, 387 (2009).
[10] Z. G. Li and G. Drazer, Phys. Rev. Lett. **98**, 050602 (2007).
[11] L. Bogunovic, M. Fliedner, R. Eichhorn, S. Wegener, J. Regtmeier, D. Anselmetti, and P. Reimann, Phys. Rev. Lett. **109**, 100603 (2012).
[12] P. T. Sharpe, *Methods of Cell Separation* (Elsevier, Amsterdam, 1988).
[13] J. Lee and A. J. C. Ladd, Phys. Rev. Lett. **89**, 104301 (2002).
[14] T. A. J. Duke and R. H. Austin, Phys. Rev. Lett. **80**, 1552 (1998).
[15] J. Han and H. G. Craighead, J. Vac. Sci. Technol. A **17**, 2142 (1999).
[16] F. Müller *et al.*, Phys. Status Solidi **182**, 585 (2000).
[17] I. Ricárdez-Vargas *et al.*, Appl. Phys. Lett. **88**, 121116 (2006).
[18] M. P. MacDonald, G. C. Spalding, and K. Dholakia, Nature (London) **426**, 421 (2003).
[19] E. Krieg *et al.*, Nature Nanotechnol. **6**, 141 (2011).
[20] J. A. Davis *et al.*, Proc. Natl. Acad. Sci. USA **103**, 14779 (2006).
[21] D. Reguera, A. Luque, P. S. Burada, G. Schmid, J. M. Rubí, and P. Hänggi, Phys. Rev. Lett. **108**, 020604 (2012).
[22] T. Motz *et al.*, J. Chem. Phys. **141**, 074104 (2014).
[23] D. Lairez, M.-C. Clochard, and J.-E. Wegrowe, Sci. Rep. **6**, 38966 (2016).
[24] B. Hille, *Ion Channels of Excitable Membranes* (Sinauer Associates, Sunderland, 1992).
[25] S. B. Chen, J. Chem. Phys. **139**, 074904 (2013).
[26] S. Martens, A. V. Straube, G. Schmid, L. Schimansky-Geier, and P. Hänggi, Phys. Rev. Lett. **110**, 010601 (2013).
[27] P. K. Ghosh, V. R. Misko, F. Marchesoni, and F. Nori, Phys. Rev. Lett. **110**, 268301 (2013).
[28] J. Happel and H. Brenner, *Low Reynolds Number Hydrodynamics: With Special Applications to Particulate Media* (Martinus Nijhoff Publishers, The Hague, 1983).
[29] M. R. Maxey and J. Riley, Phys. Fluids **26**, 883 (1983).
[30] P. Reimann, Phys. Rep. **361**, 57 (2002).
[31] R. D. Astumian and M. Bier, Phys. Rev. Lett. **72**, 1766 (1994).
[32] B. Q. Ai, Phys. Rev. E **80**, 011113 (2009).
[33] D. Reguera, G. Schmid, P. S. Burada, J. M. Rubí, P. Reimann, and P. Hänggi, Phys. Rev. Lett. **96**, 130603 (2006).
[34] M. H. Jacobs, *Diffusion Processes* (Springer-Verlag, New York, 1967).